

Endostatin inhibits the proliferation and migration of B16 cells by inducing macrophage polarity to M1-type

HUA GUO¹, LONGYUAN ZHOU², JUN GUO³, XUEQIN HUANG¹ and JUNLIAN GU⁴

¹Department of Pathology and Pathogen Biology, Ningbo University School of Medical; ²Department of Anesthesiology, Ningbo Medical Center Lihuili Hospital, Ningbo, Zhejiang 315211; ³Department of Pathology, Sanquan College of Xinxiang Medical University, Xinxiang, Henan 453000; ⁴School of Nursing and Rehabilitation, Cheeloo College of Medicine, Shangdong University, Jinan, Shandong 250012, P.R. China

Received December 3, 2020; Accepted April 23, 2021

DOI: 10.3892/mmr.2021.12481

Abstract. Malignant melanoma is a common skin tumor that easily metastasizes and has a poor prognosis. Endostatin is an endogenous vascular endothelial inhibitor that mainly suppresses tumor growth by inhibiting the proliferation of vascular endothelial cells and by reducing the formation of tumor microvessels, however the immunological function of endostatin remains unclear. Previously, we have found that an over-expression endostatin (pEndostatin) plasmid induced RAW264.7 cells' polarity to M1-type macrophage. To elucidate the effect of M1-type macrophages induced by endostatin on melanoma B16 cells, the present study transfected RAW264.7 cells with pEndostatin plasmid and co-cultured them with B16 cells. Compared with the control group, the expression of matrix metalloproteinase (MMP)-2, MMP-9 and proliferating cell nuclear antigen in B16 cells was inhibited by M1-type macrophages, but cleaved Caspase-3 and cleaved Caspase-8 were significantly upregulated and the ratio of Bax/Bcl-2 was increased. These results indicated that M1 macrophages induced by pEndostatin plasmid inhibited the proliferation and migration of B16 cells and promoted their apoptosis. These findings suggest that the inhibitory effect of endostatin on melanoma is not limited to directly inhibiting tumor

microvessel formation, but it may also be related to regulating changes in macrophage polarity.

Introduction

Malignant melanoma (MM) is one of the tumors with the highest mortality rate due to its strong invasiveness and drug resistance. In the United States, the mortality of MM has decreased upon use of new targeted therapies, but its incidence is rising (1,2). Melanoma is considered as an immunogenic tumor and its occurrence and development are affected by the interaction of various immune cells in the tumor microenvironment (TME) (3). There are several immune cells in the TME, including CD8⁺ T cells, NK cells and tumor-associated macrophages (TAMs), with TAMs being the largest proportion (4).

Macrophages can be polarized to classically activated macrophages (M1-type) or alternatively activated macrophages (M2-type). M1-type macrophages have a strong antigen presenting function that secretes a large amount of inflammatory cytokines. Furthermore, they participate in the Th1-type immune response, exert an anti-tumor immune function and inhibit tumor development (5). TAMs are thought to more closely resemble M2-type macrophages, which produce higher levels of anti-inflammatory cytokines and angiogenic factors. These factors inhibit the anti-tumor immune response and help tumor cells escape from the immune system and reactivate epithelial-mesenchymal transition (EMT) to promote tumor metastasis (6), resulting in the promotion of tumor growth and metastasis. Therefore, altering the polarity of TAMs and reprogramming them toward M1-type has become a potential target for tumor immunotherapy.

Endostatin is one of the potential endogenous angiogenesis inhibitors, which can effectively inhibit tumor angiogenesis (7), but there are few studies on its immunology. In China, the endostatin recombinant protein, Endostar, has been listed as the preferred anti-tumor angiogenesis-targeted drug for MM first-line treatment. Previously we have found that an overexpression endostatin plasmid (pEndostatin plasmid) induced M1-type polarization of mouse RAW264.7 macrophages and inhibited the growth of breast cancer (8). Therefore, it was hypothesized that M1-type macrophages

Correspondence to: Professor Junlian Gu, School of Nursing and Rehabilitation, Cheeloo College of Medicine, Shangdong University, 44 Wenhua West Road, Jinan, Shandong 250012, P.R. China
E-mail: junlian_gu@sdu.edu.cn

Abbreviations: FBS, fetal bovine serum; M1, classical activation macrophage; M2, alternative activation macrophage; MM, malignant melanoma; MMP, Matrix metalloproteinase; MTT, 3-(4, 5-dimethylthiazol-2-yl)-2, 5-dimethyltetrazolium bromide; PCNA, proliferating cell nuclear antigen; pEndostatin, the plasmid of over-express endostatin; TME, tumor microenvironment; TAMs, tumor-associated macrophages

Key words: endostatin, B16 cells, M1-type macrophages, M2-type macrophages, tumor-associated macrophages

induced by pEndostatin plasmid would also have an inhibitory effect on melanoma cells. To confirm this hypothesis, normal RAW264.7 cells or M1-type macrophages induced by pEndostatin plasmid were co-cultured with melanoma B16 cells and the changes in the biological functions of the co-cultured B16 cells were observed.

Materials and methods

Cell lines and cell culture. The mouse melanoma cell line, B16 and the mouse macrophage cell line, RAW264.7, were purchased from the Cell Bank of the Chinese Academy of Sciences. B16 cells and RAW264.7 cells were cultured in DMEM (HyClone; Cytiva) with 10% FBS (HyClone; Cytiva) and penicillin-streptomycin (1,000 $\mu\text{g/ml}$). The two cell lines were cultured at 37°C in a cell incubator with 5% CO₂.

Plasmid. To overexpress endostatin, the pcDNA3.1-ssEndostatin (pEndostatin) plasmid was constructed by the Laboratory of Pathophysiology, Basic Medical College of Jilin University, as previously described (9). The plasmid was transfected into RAW264.7 cells using Lipofectamine® 2000 (Invitrogen; Thermo Fisher Scientific, Inc.) according to the manufacturer's instructions. RAW264.7 cells were collected 48 h after transfection and then co-cultured with B16 cells.

Cell co-culture. B16 cells were inoculated into the lower chambers of Transwell 6-well plates (Corning Inc.) at a density of 5×10^5 cells/well. RAW264.7 cells or M1-type macrophages induced by pEndostatin plasmid were seeded in the upper chambers of the Transwell plates at a density of 5×10^4 cells/well. These cells were co-cultured for 48 h at 37°C in a 5% CO₂ cell culture incubator.

MTT assay. Co-cultured B16 cells were seeded in a 96-well plate at a density of 1x10⁴ cells/100 μl /well, with five replicate wells in each group and continued to be cultured for 24, 48 and 72 h. Then 20 μl MTT (5 mg/ml; Sangon Biotech Co., Ltd.) was added to each well for 4 h in the incubator. The supernatant was removed and 150 μl /well of DMSO (Sangon Biotech Co., Ltd.) was added. The light absorption of each well was measured at 490 nm by an ELISA reader and the survival rate of B16 cells was calculated.

Colony-forming cell assay. Co-cultured B16 cells were seeded in a 6-well plate at a density of 500 cells/well. After 7 days, the number of colonies (containing ≥ 50 cells) in each well was counted by crystal violet staining (Sangon Biotech Co., Ltd.). Colony-forming rate (%) = (total number of colonies/total number of seeded cells) x100.

Scratch wound assay. B16 cells co-cultured with different macrophages for 48 h were seeded in a 24-well plate and cultured overnight. When the confluence of cells was 90-100%, a scratch was applied with a 200- μl pipette tip. The wells were then rinsed twice with PBS (Hyclone, GE Healthcare Life Sciences) to wash away suspended cells and debris and the remaining cells were further cultured in DMEM with 2% FBS, which was used to maintain cell survival but prevent cell proliferation. The change in scratch

width at 0, 24 and 48 h was monitored under a BX41-PHD-P11 light microscope (Olympus Corporation). Data analyses were conducted using ImageJ (v1.8.0 National Institutes of Health). Transport rate (%) = (0 h scratch width - scratch width after cultivation)/0 h scratch width x100.

Transwell assay. Co-cultured B16 cells were inoculated (1×10^3) with normal cell culture medium into the upper chambers of Transwell plates (pore size, 8 μm), and Matrix gel (Corning Inc.), which was used for precoating at 37°C for 2 h, and normal cell culture medium was added to the lower chamber. After culturing for 24 h at 37°C, the cells on the upper chamber membrane were gently wiped with a cotton swab and then stained with crystal violet at room temperature for 20 min. The number of cells passing through the Transwell membrane was counted using a BX41-PHD-P11 light microscope (Olympus Corporation). The relative invasion rate of B16 cells in the M1 group was calculated relative to the control group. Relative invasion rate = Number of migrating cells in the M1 group/number of migrating cells in the control group.

Flow cytometry analysis. Co-cultured B16 cells were stained with an Annexin V Apoptosis kit (Beckman Coulter, Inc.) according to the manufacturer's protocol. The apoptotic ratio (late apoptosis) of each group of cells was determined by an Epics-XL-MCL flow cytometer (Beckman Coulter, Inc.). The cell cycle distribution of the co-cultured B16 cells was determined by single staining with 100 $\mu\text{g/ml}$ propidium iodide (Beckman Coulter, Inc.) at 37°C for 30 min. The fixative used for the cell cycle assay was 75% ice ethanol, overnight at -20°C.

Western blot analysis. Co-cultured B16 cells were harvested and lysed with RIPA lysis buffer (Takara Bio Inc.) and the supernatant was collected. The protein concentration was measured by a Bio-Rad protein concentration quantification method (Bio-Rad Laboratories Inc.). The protein samples (30 μg) were electrophoresed on 12% SDS-PAGE gels and transferred to PVDF membranes (Invitrogen; Thermo Fisher Scientific, Inc.), blocked with 5% skimmed milk (EMD Millipore) at room temperature for 1 h, incubated with primary antibodies overnight at 4°C and then incubated with secondary antibodies at room temperature for 1 h. Protein bands were visualized with an ECL kit (GE Healthcare). The images were captured using a Syngene Bio Imaging System (SynGene). The following primary antibodies were used: mouse monoclonal anti-matrix metalloproteinase (MMP)-2 (1:200; cat. no. sc-13594), mouse monoclonal anti-MMP-9 (1:200; cat. no. sc-21733; both Santa Cruz Biotechnology, Inc.); mouse monoclonal anti-cleaved Caspase-8 (1:1,000; cat. no. 9429), rabbit polyclonal anti-cleaved Caspase-3 (1:1,000; cat. no. 9664), rabbit polyclonal anti-proliferating cell nuclear antigen [(PCNA); 1:1,000; cat. no. 13110; all Cell Signaling Technology, Inc.]; rabbit polyclonal anti-Bax (1:500; cat. no. BS2538), rabbit polyclonal anti-Bcl-2 (1:500; cat. no. BS1511), rabbit polyclonal anti- β -actin (1:5000; cat. no. AP0060) and rabbit polyclonal anti-GAPDH (1:10,000; cat. no. AP0063; all Bioworld Technology, Inc.). The secondary antibodies used were anti-rabbit IgG (1:3,000; cat. no. sc-2357) and anti-mouse IgG (1:2,000, sc-2005; both Santa Cruz

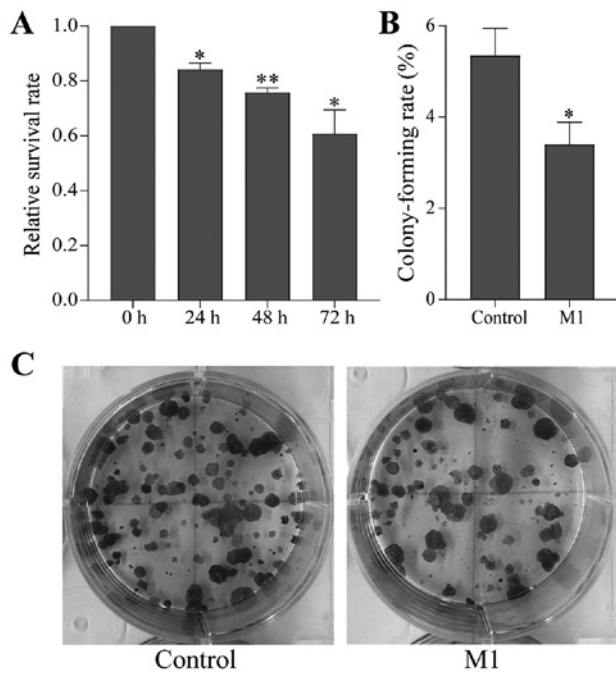


Figure 1. M1-type macrophages induced by the pEndostatin plasmid inhibit the proliferation of B16 cells. (A) MTT assay, relative survival rate of B16 cells at different time points. (B and C) Colony-forming assay tested the proliferation ability of individual cells. The data are expressed as mean \pm standard deviation. * $P < 0.05$ vs. control group; ** $P < 0.01$ vs. control group. M1, classical activation macrophage.

Biotechnology, Inc.). Protein expression was semi-quantified using ImageJ software (v1.8.0; National Institutes of Health).

Statistical analysis. The results are expressed as mean \pm standard deviation. Comparisons between two groups were analyzed using an unpaired Student's *t*-test. Comparisons among more than two groups were assessed using one-way ANOVA followed by Tukey's post hoc test in pair-wise repetitive comparisons. Data analyses were conducted using SPSS 11.0 (SPSS, Inc.). Graphs were prepared using GraphPad Prism 8 (GraphPad Software, Inc.). Each experiment was repeated three independent times. $P < 0.05$ was considered to indicate a statistically significant difference.

Results

The present study established a co-culture system with Transwell chambers. B16 cells were co-cultured with normal RAW264.7 cells (control group) or M1-type macrophages (M1 group) induced by pEndostatin plasmid for 48 h and then collected to examine their biological functions.

Endostatin-induced M1-type macrophages inhibit the proliferation of B16 cells. B16 cells co-cultured with normal RAW264.7 cells or M1-type macrophages for 48 h were collected and seeded in 96-well plates. The proliferation of the co-cultured B16 cells was determined by the MTT assay after 24, 48 and 72 h. The proliferative ability of B16 cells in the M1 group was significantly weakened and the survival rate decreased in a time-dependent manner compared with the control group (Fig. 1A).

Furthermore, the proliferation ability of individual cells was tested by the colony-forming cell assay. It was found that the colony formation ability of B16 cells in the M1 group was also reduced compared with the control group (Fig. 1B and C). This result was consistent with the MTT assay, indicating that M1-type macrophages induced by the pEndostatin plasmid inhibited the proliferation of B16 cells.

Endostatin-induced M1-type macrophages inhibit the migration and invasion of B16 cells. To examine the effect of M1-type macrophages induced by the pEndostatin plasmid on the migration and invasion of B16 cells, scratch and Transwell assays were used. After 24 and 48 h of culture, the number of B16 cells in the M1 group passing through the Transwell membrane was significantly smaller than that in the control group (Fig. 2A and B). Additionally, the scratch width of the B16 cells in the M1 group was significantly larger than that in the control group, i.e., the migration distance was reduced (Fig. 2C and D).

Next, the expression of MMPs was examined by western blotting. Compared with the control group, the expression of PCNA, MMP-2 and MMP-9 in B16 cells of the M1 group was downregulated ($P < 0.05$; Fig. 3). These results suggested that M1-type macrophages induced by the pEndostatin plasmid inhibited the migration and invasion of B16 cells by down-regulating the expression of PCNA, MMP-2 and MMP-9.

Endostatin-induced M1-type macrophages promote apoptosis of B16 cells. To further elucidate the mechanism by which endostatin-induced M1-type macrophages inhibit the proliferation of B16 cells, the changes in the cell cycle distribution and apoptosis of B16 cells were examined by flow cytometry. The results showed that the cell cycle distribution of B16 cells in the M1 group was similar to that of the control group (Fig. 4A and B), but the proportion of apoptotic cells was significantly increased (control group: $8.30 \pm 2.91\%$ vs. M1 group: $17.48 \pm 2.89\%$; $P < 0.05$; Fig. 4C and D).

Using western blotting to determine the expression of apoptosis-related proteins, it was found that the protein expression of cleaved Caspase-3 and cleaved Caspase-8 was significantly upregulated and the Bax/Bcl-2 ratio was significantly increased in B16 cells of the M1 group, compared with the control group ($P < 0.01$; Fig. 5). These results suggest that the M1-type macrophages induced by the pEndostatin plasmid inhibited the proliferation of B16 cells by promoting apoptosis, though they did not affect the cell cycle of B16 cells.

Discussion

MM has become a major public health threat owing to its high metastasis rate, drug resistance and poor prognosis (10). Although much effort has been put into the development of MM treatments in recent years, effective treatment remains limited. MM is an immunogenic tumor and its biological behavior is affected by host immune cells and inflammatory cells in the TME (3). The immunosuppressive TME composed of regulatory T cells, bone marrow-derived suppressor cells and TAMs promote the immune escape of melanoma (11,12), hence a number of researchers are beginning to investigate to MM immunotherapy. As the main immune cells in the TME

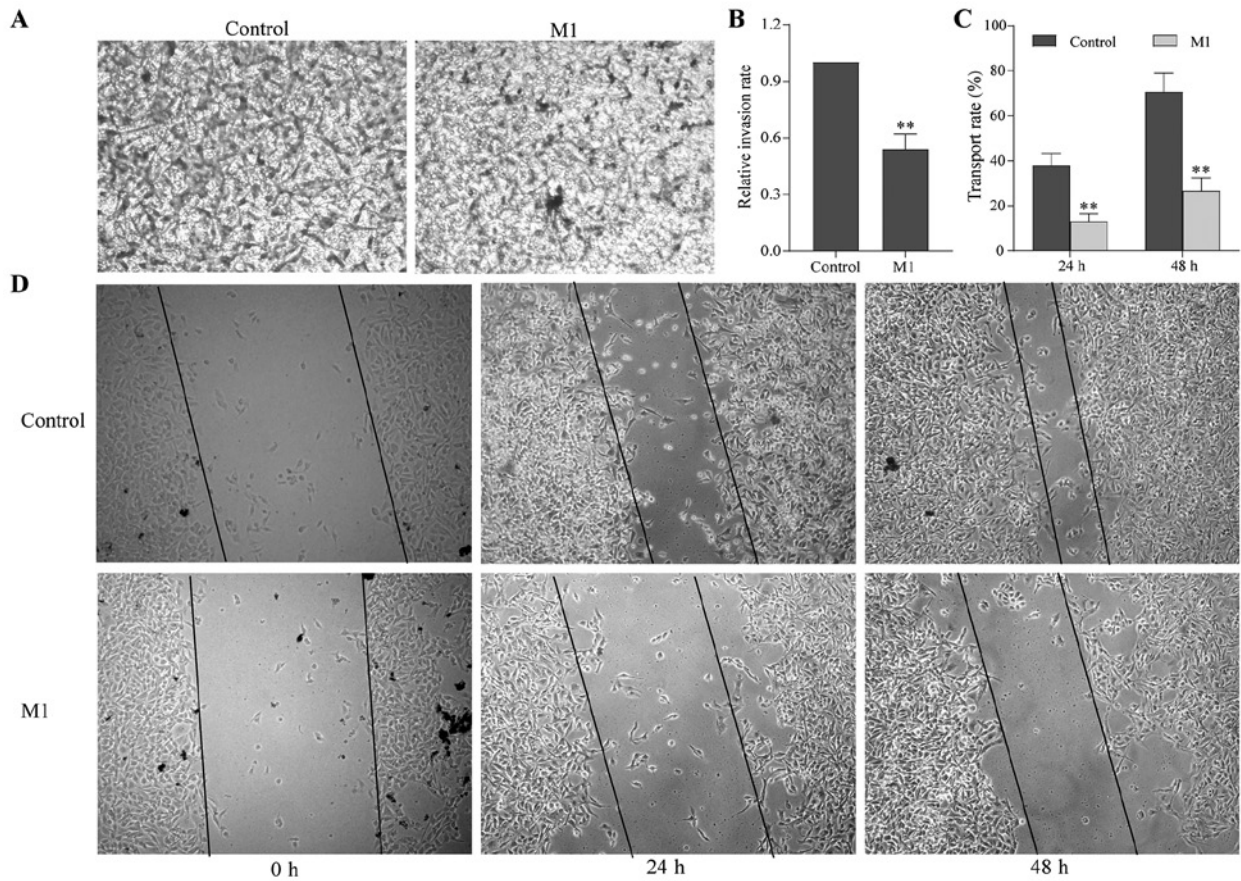


Figure 2. Endostatin-induced M1-type macrophages inhibit the migration and invasion of B16 cells. (A and B) Invasion ability as evaluated by Transwell assay (magnification, x200). (C and D) Migration ability as tested by the scratch wound assay (magnification, x100). The data are expressed as mean \pm standard deviation. ** $P < 0.01$ vs. control group. M1, classical activation macrophage.

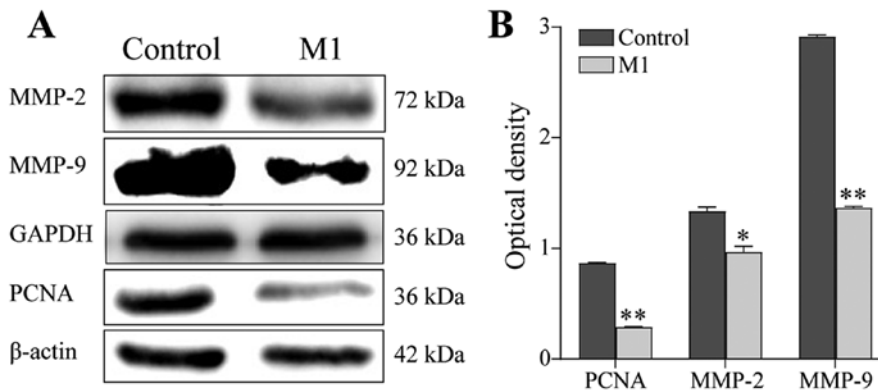


Figure 3. Effect of M1-type macrophages induced by the pEndostatin plasmid on migration-related proteins in B16 cells. The expression of PCNA, MMP-2 and MMP-9 was detected by (A) western blotting and (B) semi-quantified as a fold-change relative to GAPDH or β -actin. * $P < 0.05$ vs. control group; ** $P < 0.01$ vs. control group. M1, classical activation macrophage; PCNA, proliferating cell nuclear antigen; MMP, matrix metalloproteinase.

of MM, TAMs play an important role in the development and metastasis of MM (10). Therefore, reprogramming the polarity of TAMs to inhibit the development of MM has become of great interest to researchers. Melanoma cells release different macrophage chemokines (including monocyte chemoattractant protein 1 and VEGF-C) to attract macrophages to the tumor site and induce their activation into M2-type TAMs to exert pro-tumor effects (10,13). In turn, M2-type TAMs secrete a number of effector molecules (including IFN- γ , cyclooxy-

genase 2 and IL-10) to promote the growth and metastasis of MM, thus forming a vicious circle (10,14). Additionally, melanoma exosomes directly induce macrophage polarization to an M1/M2 'mixed' phenotype, which has multiple tumor-promoting functions (15). The immunosuppressive function of TAMs derives from their kinase activity and secretion of anti-inflammatory cytokines, including IL-10 and TGF- β , which have an inhibitory effect on tumoricidal lymphocytes. TGF- β 1 secreted by M2-type TAMs inhibits the

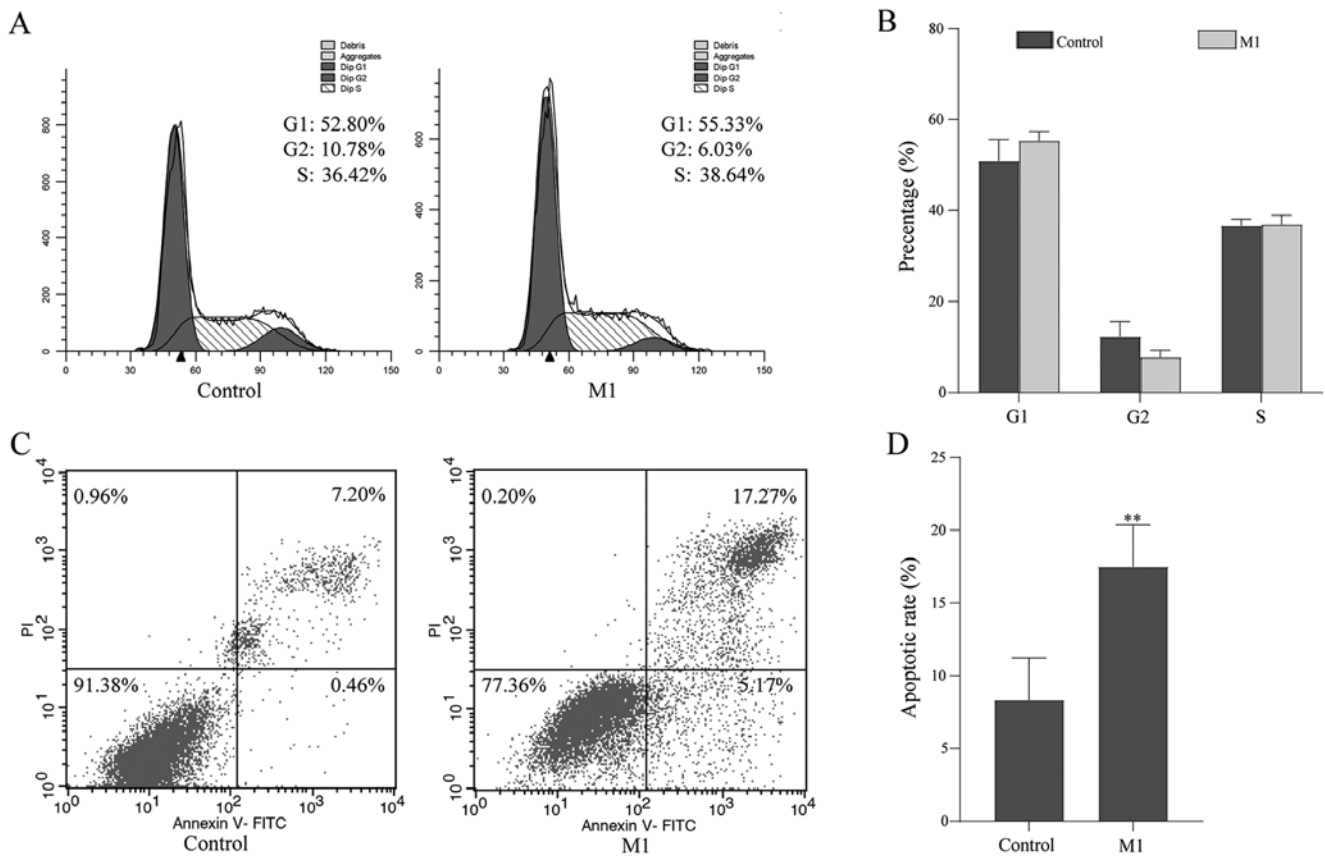


Figure 4. Effects of M1-type macrophages induced by the pEndostatin plasmid on apoptosis and the cell cycle distribution of B16 cells were examined by flow cytometry analysis. (A and B) The cell cycle distribution of B16 cells in different groups. (C and D) Apoptotic rate of B16 cells. The data are expressed as mean \pm standard deviation. **P<0.01 vs. control group.

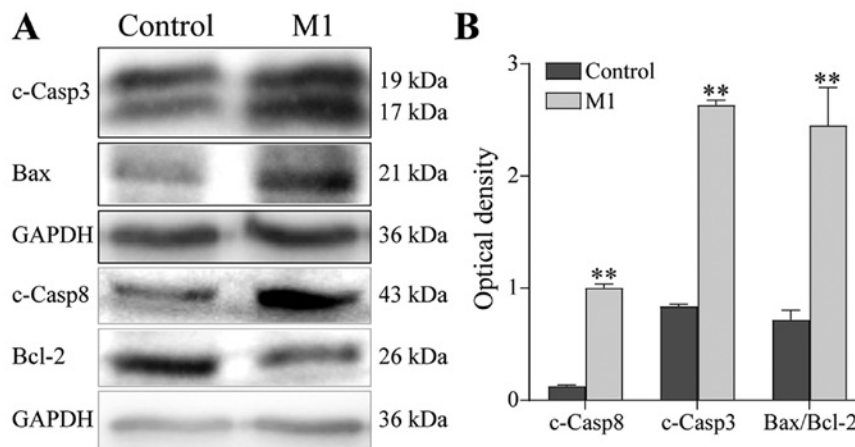


Figure 5. Effect of M1-type macrophages induced by the pEndostatin plasmid on apoptosis-related proteins in B16 cells. The expression of, c-Casp-3, c-Casp-8, Bax and Bcl-2 was detected by (A) western blotting and (B) semi-quantified as a fold-change relative to GAPDH. **P<0.01 vs. control group. M1, classical activation macrophage; c-Casp, cleaved Caspase.

release of nitric oxide from M1 macrophages (16) and inhibits M1 polarization through matrix remodeling to increase the survival of melanoma (17). Adrenomedullin produced by TAMs induces nitric oxide production in endothelial cells through a paracrine mechanism and polarizes macrophages toward M2-type through an autocrine mechanism, thereby increasing angiogenesis and tumor growth in melanoma (18). TAMs also directly activate the VEGF pathway and IL-6

secreted by TAMs promotes the generation of tumor microvessels by activating STAT3 to induce hypoxia-inducible factor 1-mediated VEGF-A transcription (19). Additionally, TAMs secrete MMPs (MMP-2, MMP-9 and MMP-7) to regulate the decomposition and reconstruction of the cell matrix, provide support for the formation of blood vessels and promote the migration of endothelial cells (20). Therefore, inducing the polarity transformation of M2-type TAMs to M1-type with

tumor suppressor function in the TME can be used as one of the targets for MM treatment. The present study found that M1 type macrophages induced by the pEndostatin plasmid inhibited the proliferation and migration of melanoma, indicating that it is feasible to treat melanoma by changing the polarity of TAMs in the TME; however, the specific mechanism requires further research.

Endostatin is an endogenous angiogenesis inhibitor isolated from the conditioned medium of hemangioendothelioma cell line (21). It suppresses tumor development by inhibiting the proliferation, migration and invasion of endothelial cells. In 2005, the State Food and Drug Administration of China approved Endostar as an anti-vascular drug for the clinical treatment of non-small cell lung cancer. As there are almost no side effects and drug resistance rarely occurs, Endostar is more suitable for patients with long-term antitumor therapy and is more effective in suppressing tumor recurrence and metastasis than other anti-vascular targeted therapies (22).

It has been demonstrated that Endostar inhibits the growth of melanoma by inhibiting angiogenesis and the MAPK pathway mediated by basic fibroblast growth factor (23). A combined treatment with Endostar and chemotherapeutics significantly inhibits the proliferation of melanoma cells and promotes their apoptosis and prolonged the survival time of tumor-bearing mice (24). Clinical trials found that treatment with Endostar + dacarbazine increased the one-year survival rate (22.5 vs. 49.7%) and the two-year survival rate (14.3 vs. 22.2%) of melanoma patients compared with the placebo + dacarbazine group and reduced the risk of death in patients with mucosal melanoma (93%) and acral melanoma (62%) (25,26). Endostar combined with dacarbazine and cisplatin was effective for MM without genetic mutations and the patient tolerated the treatment well (27). Additionally, endostatin may be used as a prognostic biomarker of immunotherapy with ipilimumab for MM patients (28). These studies suggest that endostatin can inhibit microvascular growth in melanoma and improve drug resistance.

Although there are a number of studies about endostatin inhibiting MM tumor microvessels, it remains unclear whether it can inhibit MM growth by regulating the polarity of macrophages. Some studies have found that endostatin enhanced the anti-tumor immune response and increased the infiltration of cytotoxic T lymphocytes to the TME and polarized the macrophages that reached the tumor tissue to M1-type, resulting in an increased proportion of M1-type TAMs and reduced proportion of M2-type TAMs, thereby reversing the immunosuppressive environment in the TME (8,29-31). From the perspective of the change of macrophage polarity, the present study briefly explored that the inhibition of endostatin on B16 cells may be partly due to its immunological function, but the specific mechanism requires further study. More in-depth studies on its related pathways (including angiogenesis factor and oxidative stress markers) are being conducted. The present study found that M1-type macrophages induced by the pEndostatin plasmid inhibited the proliferation of B16 cells by promoting apoptosis and inhibited their migration and invasion ability by downregulating the expression of MMP-2 and MMP-9. These results suggested that in addition to directly inhibiting the formation of microvessels in MM, the therapeutic effect

of endostatin on MM was also related to inducing a polarity change in TAMs.

Acknowledgements

Not applicable.

Funding

The present study was supported by the Natural Science Foundation of Zhejiang Province (grant nos. LQ20H160009 and LY18H280004), the Natural Science Foundation of Ningbo (grant no. 2019A610318) and K.C. Wong Magna Fund in Ningbo University.

Availability of data and materials

The datasets used and/or analyzed during the current study are available from the corresponding author on reasonable request.

Authors' contributions

JGu participated in project design and technical guidance. HG participated in project design and was a major contributor to writing the manuscript and data analysis. LZ performed the investigation of B16 cell proliferation, migration and apoptosis. JGuo performed the western blotting. XH performed the investigation of B16 cell invasion. XH and HG confirmed the authenticity of all the raw data. All authors reviewed and approved the final manuscript.

Ethics approval and consent to participate

Not applicable

Patient consent for publication

Not applicable

Competing interests

The authors declare that they have no competing interests

References

1. Henley SJ, Ward EM, Scott S, Ma J, Anderson RN, Firth AU, Thomas CC, Islami F, Weir HK, Lewis DR, *et al*: Annual report to the nation on the status of cancer, part I: National cancer statistics. *Cancer* 126: 2225-2249, 2020.
2. Upreti D, Bista A, Chennamadhavuni A, Niroula A, Jafri SIM, Smith A and Arjyal L: Survival trends among patients with metastatic melanoma in the pretargeted and the post-targeted era: A US population-based study. *Melanoma Res* 28: 56-60, 2018.
3. Ladányi A: Prognostic and predictive significance of immune cells infiltrating cutaneous melanoma. *Pigment Cell Melanoma Res* 28: 490-500, 2015.
4. Yang L and Zhang Y: Tumor-associated macrophages: From basic research to clinical application. *J Hematol Oncol* 10: 58, 2017.
5. Mantovani A, Sica A, Sozzani S, Allavena P, Vecchi A and Locati M: The chemokine system in diverse forms of macrophage activation and polarization. *Trends Immunol* 25: 677-686, 2004.
6. Fuxe J and Karlsson MC: TGF- β -induced epithelial-mesenchymal transition: A link between cancer and inflammation. *Semin Cancer Biol* 22: 455-461, 2012.

7. Walia A, Yang JF, Huang YH, Rosenblatt MI, Chang JH and Azar DT: Endostatin's emerging roles in angiogenesis, lymphangiogenesis, disease, and clinical applications. *Biochim Biophys Acta* 1850: 2422-2438, 2015.
8. Guo H, Liu Y, Gu J, Wang Y, Liu L, Zhang P and Li Y: Endostatin inhibits the growth and migration of 4T1 mouse breast cancer cells by skewing macrophage polarity toward the M1 phenotype. *Cancer Immunol Immunother* 65: 677-688, 2016.
9. Jia H, Li Y, Zhao T, Li X, Hu J, Yin D, Guo B, Kopecko DJ, Zhao X, Zhang L, *et al*: Antitumor effects of Stat3-siRNA and endostatin combined therapies, delivered by attenuated *Salmonella*, on orthotopically implanted hepatocarcinoma. *Cancer Immunol Immunother* 61: 1977-1987, 2012.
10. Wang H, Yang L, Wang D, Zhang Q and Zhang L: Pro-tumor activities of macrophages in the progression of melanoma. *Hum Vaccin Immunother* 13: 1556-1562, 2017.
11. Umansky V and Sevko A: Tumor microenvironment and myeloid-derived suppressor cells. *Cancer Microenviron* 6: 169-177, 2013.
12. Ruffell B and Coussens LM: Macrophages and therapeutic resistance in cancer. *Cancer Cell* 27: 462-472, 2015.
13. Skobe M, Hamberg LM, Hawighorst T, Schirner M, Wolf GL, Alitalo K and Detmar M: Concurrent induction of lymphangiogenesis, angiogenesis, and macrophage recruitment by vascular endothelial growth factor-C in melanoma. *Am J Pathol* 159: 893-903, 2001.
14. Wang H, Zhang L, Yang L, Liu C, Zhang Q and Zhang L: Targeting macrophage anti-tumor activity to suppress melanoma progression. *Oncotarget* 8: 18486-18496, 2017.
15. Bardi GT, Smith MA and Hood JL: Melanoma exosomes promote mixed M1 and M2 macrophage polarization. *Cytokine* 105: 63-72, 2018.
16. Vodovotz Y, Bogdan C, Paik J, Xie QW and Nathan C: Mechanisms of suppression of macrophage nitric oxide release by transforming growth factor beta. *J Exp Med* 178: 605-613, 1993.
17. Berking C, Takemoto R, Schaidler H, Showe L, Satyamoorthy K, Robbins P and Herlyn M: Transforming growth factor-beta1 increases survival of human melanoma through stroma remodeling. *Cancer Res* 61: 8306-8316, 2001.
18. Chen P, Huang Y, Bong R, Ding Y, Song N, Wang X, Song X and Luo Y: Tumor-associated macrophages promote angiogenesis and melanoma growth via adrenomedullin in a paracrine and autocrine manner. *Clin Cancer Res* 17: 7230-7239, 2011.
19. Xu Q, Briggs J, Park S, Niu G, Kortylewski M, Zhang S, Gritsko T, Turkson J, Kay H, Semenza GL, *et al*: Targeting Stat3 blocks both HIF-1 and VEGF expression induced by multiple oncogenic growth signaling pathways. *Oncogene* 24: 5552-5560, 2005.
20. Murdoch C, Muthana M, Coffelt SB and Lewis CE: The role of myeloid cells in the promotion of tumour angiogenesis. *Nat Rev Cancer* 8: 618-631, 2008.
21. O'Reilly MS, Boehm T, Shing Y, Fukai N, Vasios G, Lane WS, Flynn E, Birkhead JR, Olsen BR and Folkman J: Endostatin: An endogenous inhibitor of angiogenesis and tumor growth. *Cell* 88: 277-285, 1997.
22. Li K, Shi M and Qin S: Current Status and Study Progress of Recombinant Human Endostatin in Cancer Treatment. *Oncol Ther* 6: 21-43, 2018.
23. Xiao L, Yang S, Hao J, Yuan X, Luo W, Jiang L, Hu Y, Fu Z, Zhang Y and Zou C: Endostar attenuates melanoma tumor growth via its interruption of b-FGF mediated angiogenesis. *Cancer Lett* 359: 148-154, 2015.
24. Zheng AW, Jia DD, Xia LM, Jin G, Wu H and Li T: Impact of carboplatin plus paclitaxel combined with endostar against A375 melanoma cells: An in vitro and in vivo analysis. *Biomed Pharmacother* 83: 1321-1326, 2016.
25. Cui C, Mao L, Chi Z, Si L, Sheng X, Kong Y, Li S, Lian B, Gu K, Tao M, *et al*: A phase II, randomized, double-blind, placebo-controlled multicenter trial of Endostar in patients with metastatic melanoma. *Mol Ther* 21: 1456-1463, 2013.
26. Cui C, Si L, Chi Z, Sheng X and Guo J: Preliminary results of a phase II trial with continuous intravenous infusion of rh-endostatin in combination with dacarbazine as the first-line therapy for metastatic acral melanoma. *Anticancer Res* 35: 4350-4351, 2015.
27. Yang L, Xu Y, Luo P, Chen S, Zhu H and Wang C: Baseline platelet counts and derived inflammatory biomarkers: Prognostic relevance in metastatic melanoma patients receiving Endostar plus dacarbazine and cisplatin. *Cancer Manag Res* 11: 3681-3690, 2019.
28. Nyakas M, Aamdal E, Jacobsen KD, Guren TK, Aamdal S, Hagene KT, Brunsvig P, Yndestad A, Halvorsen B, Tasken KA, *et al*: Prognostic biomarkers for immunotherapy with ipilimumab in metastatic melanoma. *Clin Exp Immunol* 197: 74-82, 2019.
29. Liu X, Nie W, Xie Q, Chen G, Li X, Jia Y, Yin B, Qu X, Li Y and Liang J: Endostatin reverses immunosuppression of the tumor microenvironment in lung carcinoma. *Oncol Lett* 15: 1874-1880, 2018.
30. Liang J, Liu X, Xie Q, Chen G, Li X, Jia Y, Yin B, Qu X and Li Y: Endostatin enhances antitumor effect of tumor antigen-pulsed dendritic cell therapy in mouse xenograft model of lung carcinoma. *Chin J Cancer Res* 28: 452-460, 2016.
31. Wang X, Zhan RY, Wang YY, Yan XI, Cao D, Li Y, Wang YQ and Luo F: Endostatin improves cancer-associated systemic syndrome in a lung cancer model. *Oncol Lett* 9: 2023-2030, 2015.